University of Twente

Bachelor's Assignment

# Probing the vibrational modes of proteins diffusing on a charged plasmonic surface

*Dynamic NanoPhotonics*
*NanoBioPhysics*
*Faculty of Science and Technology*

*Okke Peters s2398397*

*Committee:*

| | |
|---|---|
| *Daily Supervisor:* | *M.R. Aghdaee (MohammadReza)* |
| *Main Supervisor:* | *dr. O.S. Ojambati (Femi)* |
| *External Member:* | *dr.ir. G. Katsoukis (Georgios)* |

January 29, 2024

# Abstract

Proteins are essential biomolecules that play vital roles in almost all biological processes. Changes in their structure, even at extremely low concentrations, have been long associated with diseases like Alzheimer's or Parkinson's. Studying and understanding the protein folding process and factors that can influence it are therefore important to be studied. Raman spectroscopy of proteins allow researchers to identify protein structure on the basis of their vibrational modes. Raman signatures are weak and thus Surface-Enhanced Raman Spectroscopy (SERS) is used widely by researchers today. SERS uses metallic nanostructures to greatly enhance the Raman signal. To increase stability of this enhanced Raman signal self-assembled monolayers are used to act as a barrier between the gold nanoparticles and the protein.

This research aims to understand the influence of the (net-)charge of proteins and their environment on their structural conformation, while in solution. In this report the Surface-Enhanced Raman Spectra of two protein solutions, containing Bovine Serum Albumin (BSA) or Lysozyme, on top of bare gold nanoparticles or a negatively charged self-assembled-monolayer are analyzed. Two gold nanoparticle aggregation protocol and a second linking molecule are also evaluated for SERS measurements in solution.

The research shows that the gold nanoparticle aggregation protocol using acetone is unsuitable for SERS measurements in solution as the acetone on top of the aggregation interferes with the signal coming from the protein, even when little acetone is used. Due to inconsistent signal appearing in dry conditions, cysteamine hydrochloride was found to be unsuitable as a self-assembled monolayer for protein solution measurements. The research does show succesful measurements with both proteins on top op an MPA self-assembled monolayer. From these measurements it was found that BSA undergoes a structural change from mostly $\alpha$-helix to a more $\beta$-sheet conformation. The negative charge of MPA was found to induce $\alpha$-helix formation in lysozyme by interacting with its positively charged side-chains.

# Contents

# 1 Introduction

Raman spectroscopy is a spectroscopic technique which can identify the structure of molecules by their molecular vibrations. When a molecule is exposed to a light source this light scattered. Over 99 % of this light is scattered elastically, keeping its initial wavelength. An extremely small fraction of this light is scattered inelastically and changes in its energy from interacting with the molecule, this is called Raman scattering. A spectrum of this Raman scattered light includes a lot of information about the structure of the molecule and can be used to identify the molecule itself or structures it contains. However, due to the incredibly small amount of light that's actually scattered inelastically it is challenging to detect weaker Raman signals.

To detect these weaker Raman signals a technique called Surface-Enhanced Raman Spectroscopy (SERS) is used. This technique utilizes small metallic nanoparticles to greatly enhance the Raman signal. The incoming light induces an oscillation of electrons around the nanoparticle, creating an enhanced electromagnetic field. Even a single nanoparticle can enhance this signal but its enhancement is far more potent when it's close to other nanoparticles. This nanoparticle coupling can enhance the signal in such a way that incredibly small concentrations of molecules can still be detected. One of the major drawbacks of SERS is the interactions between the nanoparticle aggregations and the biomolecule being measured. Some biomolecules can denature or change structure when in close contact with the metallic structures, thus changing the Raman signal. To decrease the interactions between the biomolecules and nanoparticles self-assembled monolayers are used as a barrier between them. These SAMs stabilize the signal and can be manipulated to create specific surface conditions, like a positive or negative charge.

For small biomolecules the use of a self-assembled monolayer is not critical in identifying its structure. When it comes to more complex molecules, however, these SAM-layers can play a critical role in identifying its structure and content. One of the main groups of these complex molecules are proteins. Proteins are a crucial part of almost all biological processes, and even a small change in its complex structure can have massive influence on its functionality. The primary structure of a protein is the long sequence of amino acids that makes up the protein. The secondary structure of a protein is characterized by the structures that form from short sequences of amino acids next to each other in the sequence that makes up the protein. The tertiary and quarternary structure describe how the individual amino acids from the primary structure and the small three-dimensional secondary structures combine together to create the full three-dimensional structure of a protein. Even extremely small concentrations of proteins with misfolded secondary structures have been linked to multiple diseases like Huntington and Alzheimer's.

Therefore it is crucial to gain insight into the protein folding process and how that's influenced by a protein's own characteristics and the characteristics of its environment. The objective of this research is to identify the changes in secondary conformation of a protein on the basis of its Surface-Enhanced Raman spectrum. This includes changing the attributes of the protein in question as well as the environment the protein is measured on. This involves fabricating samples, applying different SAM-layers and analyzing different proteins with different secondary conformations and charges to determine how the protein and SAM-layer interact.

## 1.1 Research Questions

The main research question for this report is: *How does a plasmonic surface modify the vibrational modes of a protein in solution?* Besides this main research question three sub-questions have been formulated to contribute to answering the main question.

- How does the net-charge of a protein influence the SERS spectrum?
- How does the secondary structure of a protein influence the SERS spectrum?
- How does a charged self-assembled monolayer influence the SERS spectrum of a (net-)charged protein?

# 2 Theoretical Background

The following section contains the theoretical background that forms the basis for the surface-enhanced Raman spectroscopy experiments performed in this research. The fundamentals of Raman Spectroscopy is summarized after which the phenomenon of surface enhancement is explained. Self-assembled monolayers and their use within SERS summarized and finally the structure, use and signature of proteins within Raman spectroscopy are defined.

## 2.1 Raman Spectroscopy

Raman spectroscopy is a spectroscopy technique that can identify molecules based on its vibrational signature. When monochromatic light falls onto an object smaller than its wavelength this light interacts with the molecule and is scattered. Most of this light is scattered with the same wavelength as the incident light, this is called elastic or Rayleigh scattering. A small fraction of the time the light interacts with the molecule and induce a change in the vibrational modes of the molecule, scattering inelastically. This inelastic scattering is called Raman scattering. The energies of these photons change depending on the changes they induce, thus changing the wavelength of the light. If the wavelength of the light decreases and the light loses energy to the molecule, it is called Stokes scattering. If the inverse is true and the light gains energy from the molecule it is called anti-Stokes scattering. The change in wavelength of the scattered photons compared to the incoming light is called the raman shift. All of the inelastically scattered light together can form a spectrum of the vibrational changes and thus structural components present in the molecule.

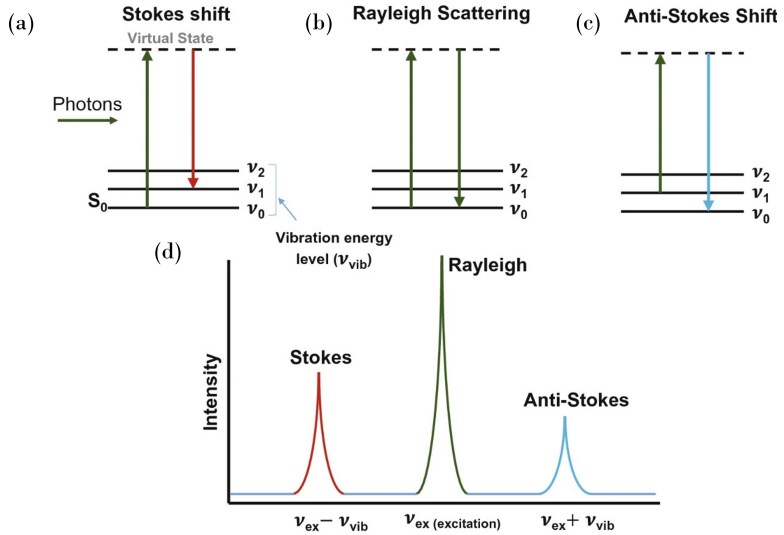


***Figure 1:*** *Energy-level diagram of (a) Stokes Raman scattering, (b) Rayleigh scattering, (c) anti-Stokes scattering. (d) Frequency comparison of Rayleigh, Stokes and Anti-Stokes scattering.*

## 2.2 Surface Enhancement

Surface Enhancement hinges on the interactions the incoming light and the small metal nanoparticles next to the biomolecule. The effect that actually induces this enhancement is called localized surface plasmon resonance. When light hits a nanoparticle smaller than its own wavelength, the electric field of the light causes an oscillation of the electrons around the surface of the nanoparticle. This oscillation of electrons in turn creates an enhanced electromagnetic field around the nanoparticle [1]. The magnitude and spectrum of the plasmonic effect is greatly influenced by the size, shape and material of a single nanoparticle [2]. In SERS measurements the scattered light from the nanoparticles is visible as a broad background without any significant peaks.

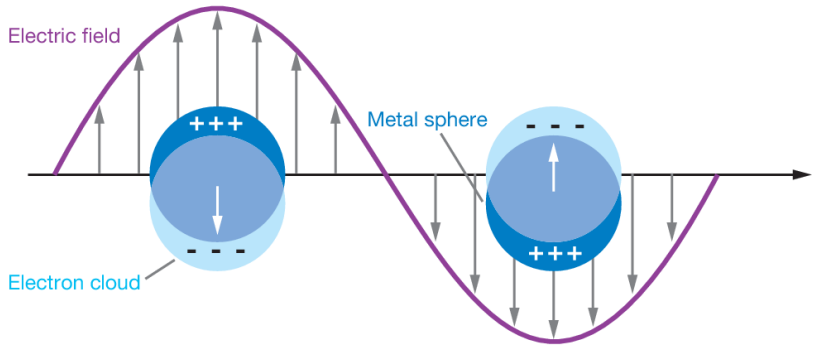


***Figure 2:*** *A schematic representation of a the localized surface plasmon effect.*

The magnitude of SERS intensity is widely approximated to be proportional to $|E(\omega_{inc})|^4$.[3]. Furthermore, the electric field strength around the nanoparticle is proportional to $r^{-3}$ [4]. This means that the SERS intensity is proportional to $r^{-12}$. It follows that it is crucial for the biomolecule to be in close contact with the nanoparticles for any SERS intensity to be captured. To quantify the role that the nanoparticle structures play in the Raman signal the Enhancement Factor (EF) can be calculated. This enhancement factor is dependant on the electric field at the enhancement site divided by the incoming electric field. Together with the fact that SERS intensity is proportional to $|E(\omega_{inc})|^4$ this creates the formula: $EF = (\frac{E_{loc}}{E_{inc}})^4$. This means that an increase of relative enhancement of ten will lead to an overall increase in SERS intensity of ten thousand [4]. The enhancement factor around one single nanoparticle in isolation is quite small. Very high SERS enhancement only occurs in the junctions inbetween nanoparticles. If the distance between two nanoparticles is small they are known as coupled. The plasmonic effect of one nanoparticle enhances the plasmonic effect of the other and vice versa, thus achieving a big increase in enhancement factor. This hotspot is the place where the best signal can be achieved. A single molecule in a perfect hotspot can give the same raman signal as 10 million molecules at a lower enhancement [4]. To increase the signal even further a monolayer aggregate of gold nanoparticles is used. This aggregation leads to a lot more hotspots in the field of view of the setup and thus a lot more enhancement. This is especially important in solution based applications. Due to the nature of measuring in a solution the protein cannot always be around the surface of the gold. Having a large aggregation with a lot of hotspots thus increases the chance of measuring an event of a protein coming close to the gold surface. Another way the Enhancement is increased is by using nanoparticle on mirror (NPoM) geometry. In this setup the gold nanoparticles are laid down on top of a thin layer of gold film. This gold film acts as a mirror which reflects the image of the charge of the nanoparticle. The nanoparticle's charge can couple with this image charge, thus even further increasing the enhancement [5].

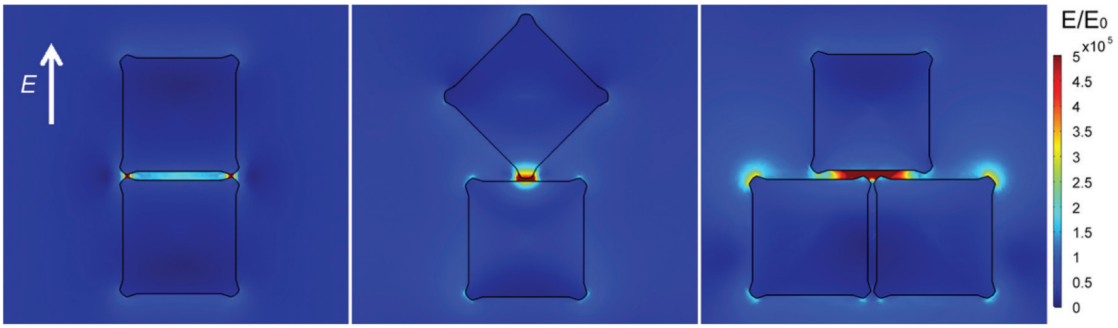


***Figure 3:*** *Simulated electric field enhancement between cube shaped nanoparticles. The arrangement on the very right displays the increase in area where a high enhancement factor is present similar to when a great amount of nanoparticles are coupled like in a larger monolayer aggregation.*

## 2.3 Self-Assembled Monolayers

A self-assembled monolayer is a layer of small molecules which is added on top of the layer of gold nanoparticles. In general these molecules are made up of a head and a tail. The head binds to the desired substrate's surface and densely fills in the entire surface of the substrate. The tails are made

up of a carbon chain of a particular length with a functional group on the other end. This functional group can have all kinds of properties dependent on the experiment being done. In the case of the SERS measurements sulfur atoms within the head of the linking molecule bind to the gold to form a monolayer [6]. Two linking molecules are used in this research. 3-Mercaptopropionic Acid (MPA) which functionalizes the gold surface with a negative charge and Cysteamine Hydrochloride which functionalizes the gold surface with a positive charge [7], [8]. Adding a SAM-layer to a SERS-substrate can greatly increase the stability of the signal. This is due to the SAM-layer acting as a robust layer in between the biomolecule and the actual gold surface. Due to this layer the interactions between the imperfections of the gold surface and the biomolecule can be prevented [9]. However, if the layer is too thick, it can greatly decrease the enhancement effect and thus signal strength.

## 2.4 Proteins and Raman

Proteins are at the basis of almost all of life's processes. Thus, even a small change in its structure can have massive effects on someone's quality of life. Protein structure is divided into four categories: primary, secondary, tertiary and quarternary. The primary structure of a protein is the sequence of amino acids that makes up the protein. The secondary structure of a protein is characterized by the structures that form from short sequences of amino acids next to each other in the sequence that makes up the protein. The most common secondary structures are the $\alpha$-helix and the $\beta$-sheets and turns. The tertiary and quarternary structure describe how the individual amino acids from the primary structure and the small three-dimensional secondary structures combine together to create the full three-dimensional structure of a protein [10]. This entire process is called protein folding. There are an incredible amount of factors that can influence the structure of a protein during and after the folding process and a lot of the protein folding process is not yet well understood. The information for the general structure of proteins is contained within the amide bands of the raman spectra. Within these bands the amide I and amide III bands are most sensitive to conformational changes of proteins [11].

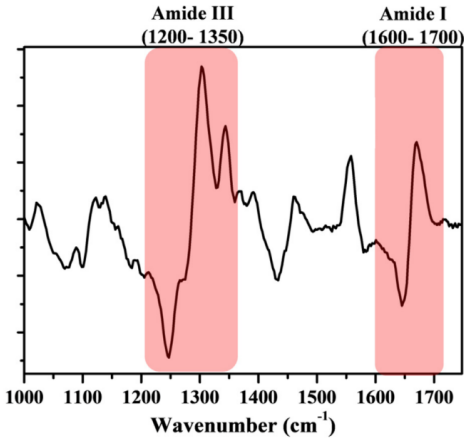


***Figure 4:*** *A Raman spectrum with indicated Amide I and Amide III bands.*

The amide I band ranges from 1600 to 1700 $cm^{-1}$ and mostly contains the C=O stretching vibrations [10]. These stretching vibrations are really sensitive to changes in the backbone conformation and are not influenced by side chains of the protein [12]. Peaks within the amide I band thus directly correlate to the secondary conformation of the protein. The amide III band ranges from 1200 to 1350 $cm^{-1}$ and is very sensitive to the secondary conformation of a protein, with distinct bands having been assigned to all major secondary structure types [11]. The amide III band however suffers from being influenced by side chains and being less pronounced than the amide I band. For the amide I peaks the following assignments have been made: The $\alpha$-helix peak is located between 1650 and 1655 $cm^{-1}$ . $\beta$-sheets will be located between 1660 and 1670 $cm^{-1}$, with a second peak between 1630 and 1635 $cm^{-1}$. A peak between 1670 and 1680 $cm^{-1}$ is assigned to $\beta$ turns [10], [12]. In the Amide III band the $\alpha$-helix structure has a peak located between 1270 and 1300 $cm^{-1}$. The $\beta$-sheets peak can be found in the range of 1230 to 1240 $cm^{-1}$. Finally random structures can be found between 1240 and 1250 $cm^{-1}$ [10], [13].

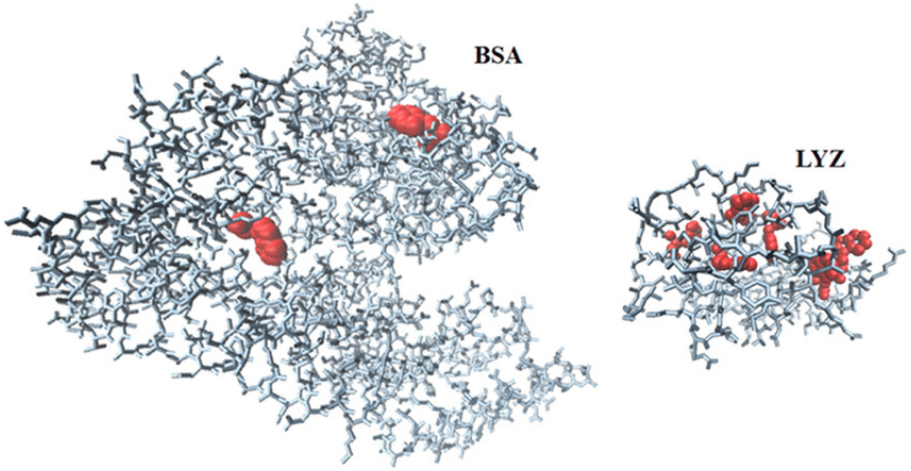


***Figure 5:*** *An Image showing a simplified representation of the 3D-structures of BSA and Lysozyme*

### 2.4.1 Bovine Serum Albumin (BSA)

Bovine Serum Albumin is one of the main proteins being studied using Raman Spectroscopy today. Its structure and composition is well understood which makes it a great candidate for research into changes of protein structure. BSA can be divided into three domains which are all negatively charged. The first two domains are especially negatively charged with a charge of $-9e$ and $-7.8e$ respectively, while the third domain only has a slight charge of $-1.3e$ [14]. This means that the net charge of this protein is also negative. Bovine Serum Albumnin has a secondary structure composed of 67 percent $\alpha$-helices and some $\beta$-structures in its regular form [10], [15]. Changes in the secondary structure of BSA can lead to protein aggregation, a phenomenon which has been linked to Alzheimer's and Huntington disease [16]. One of the pathways through which BSA can form aggregates is through the conversion of $\alpha$-helix structures to $\beta$-sheets [17]. For BSA the amide I peak, attributed to its $\alpha$-helix content, is located at 1653 $cm^{-1}$. BSA also contains a couple amino acid residues in its structure, namely: phenylalanine, tryptophan and tyrosine [18]. Within the interested range phenylalanine has peaks at 1586 and 1606 $cm^{-1}$[19]. The location of the tryptophan peak is dependant on the torsion angle within the amino acid side group, the average of this range lies at 1550 $cm^{-1}$ [10], [20]. Tyrosine is represented by a peak around 1613 $cm^{-1}$, with a peak at 1620 $cm^{-1}$ in a BSA spectrum [21].

### 2.4.2 Lysozyme

Lysozyme is a protein which is present in most living organisms that is widely studied using Raman Spectroscopy as well. Its concentration within the human body is usually quite low. However, both higher and lower levels of lysozyme in the human body and urine is associated with diseases like leukemia [22], [23]. Thus, sensitive and accurate detection of lysozyme is one of the fields of study where Raman spectroscopy is used. Lysozyme has a secondary structure composed of 40 percent $\alpha$-helix structures and a lot more random structures compared to BSA [24]. Lysozyme has an isoelectric point of 11, making it positively charged compared to BSA's negative charge [25]. When it comes to amino acid residues lysozyme contains many more Tryptophan groups than BSA and contains only 3 Phenylalanine residues compared to the 24 BSA contains [10]. These differences in protein structure makes lysozyme an interesting counterpart to BSA for this research.

# 3 Experimental Methods

## 3.1 Sample Fabrication

### 3.1.1 Template stripping

The sample fabrication process starts with the gold film. To manufacture a relatively large, flat gold surface for the gold nanoparticles to aggregate on the template stripping method is used. First, gold is deposited on an ultrasmooth surface made from silicon. This leaves an ultrasmooth bottom surface and a rough top surface. Epoxy is put on top of the rough gold surface and a small glass cover slip is added. After the epoxy has been hardened the sample can be removed from the silicon wafer. After the sample is flipped, an ultrasmooth gold surface will be left on top.

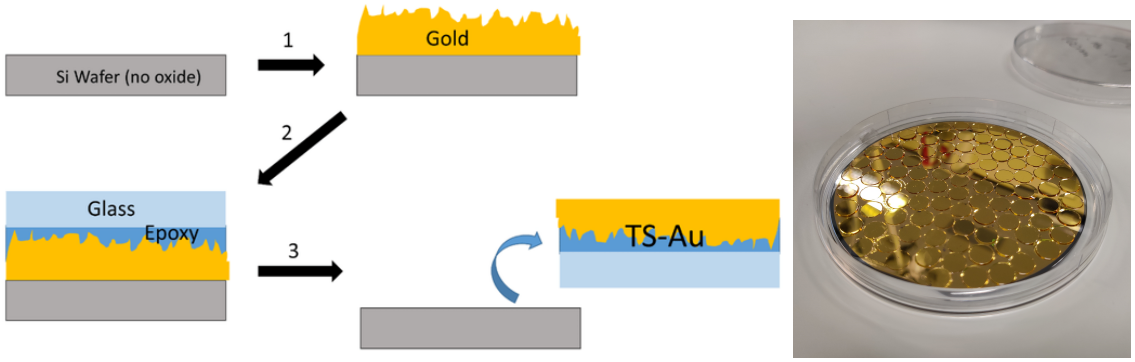


*(a)* *(b)*

***Figure 6:*** ***(a)****: a visual representation of the template stripping procedure;* ***(b)****: a picture of the gold film after the epoxy has been hardened.*

### 3.1.2 Gold nanoparticle aggregation

In this report two different gold nanoparticle aggregation protocols are used. The general process of fabrication gold nanopartical agggregates is as follows: The gold nanoparticles are stripped from the citrates that surrounds them. They are then mixed with butylamine to ensure that the gold nanoparticles can bond together. A layer of hexane is added on top of the gold nanoparticle butylamine mixture. The gold nanoparticles now form a single layer of aggregates on the interface between the hexane and the gold nanoparticle butylamine solution. This layer of aggregation is then used to cover the thin gold film, creating the sample that can be used for SERS.

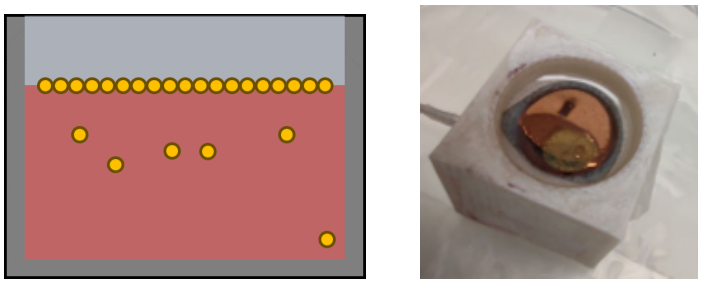

*(a)* *(b)*

***Figure 7:*** ***(a)****: A visual representation of the nanoparticles aggregating on the interface between the hexane (gray) and the gold nanoparticle and butylamine solution (red);* ***(b)****: A picture of the gold layer, with a copper-like colour, on the interface.*

**Protocol 1**

Mix 1.0 $mL$ of gold nanoparticle solution and 1.0 $mL$ of acetone in a safe-lock tube. Centrifuge this mixture for 10 minutes at 5000 RCF. Remove 1.0 $mL$ of the supernatant and mix the remaining solution thoroughly. Add 1.0 $mL$ of a 3 $mM$ butalymine solution and mix. Leave this mixture for 10 minutes. Add the 2.0 $mL$ of the mixture to the chamber. Gently add 1.0 $mL$ of hexane on top of the mixture to form a top layer. Add 1.0 $mL$ of acetone quickly and consistently through the hexane layer. Wait until a gold layer is visible just under the top surface. To apply this gold layer to the gold film, first really carefully remove around 0.25 $mL$ of solution from the top surface. Then, pick up the gold film sample

with tweezers and put it into the chamber. Pull the sample out of the chamber carefully as to cover the sample with the gold layer and let it dry.

**Protocol 2**
Attach a gold film sample to the bottom of a 3d-printed chamber using carbon-tape. Mix 1.0 $mL$ of gold nanoparticle solution and 1.0 $mL$ of ethanol in a safe-lock tube. Centrifuge this mixture until the nanoparticles are all collected in a single spot and the rest of the solution is clear. Remove 1.0 $mL$ of the supernatant and mix the remaining solution thoroughly. Add this solution to the chamber directly on top of the gold film. Secondly, add a mixture of 0.5 $mL$ 3 $mM$ butylamine solution and 0.5 $mL$ of ethanol to the side of the chamber. Finally add 1.0 $mL$ of pure hexane to the side of the chamber and mix the solution until the solution is cloudy and evenly mixed. Cover the chamber for 2 hours, after which the chamber is connected to a pump which removes 0.1 $mL$ of solution from the chamber until it's empty. When the top of the sample is completetly dry it can be removed from the chamber and used for experiments.

### 3.1.3 Adding a self-assembled monolayer

After the gold nanoparticles have aggregated on the gold film a self-assembled monolayer can be added on top. To do this the chosen linking molecule is soaked on the surface. First, the sample is put in a small glass jar. Second, 1.0 $mL$ of a 1 $mM$ linking molecule solution is added on top of the sample, making sure the sample stays on the bottom surface. The sample is soaked overnight, about 15 hours, to make sure the monolayer can form. Afterwards the sample can be taken out of the jar, rinsed with the solvent of the linking molecule and dried with nitrogen.

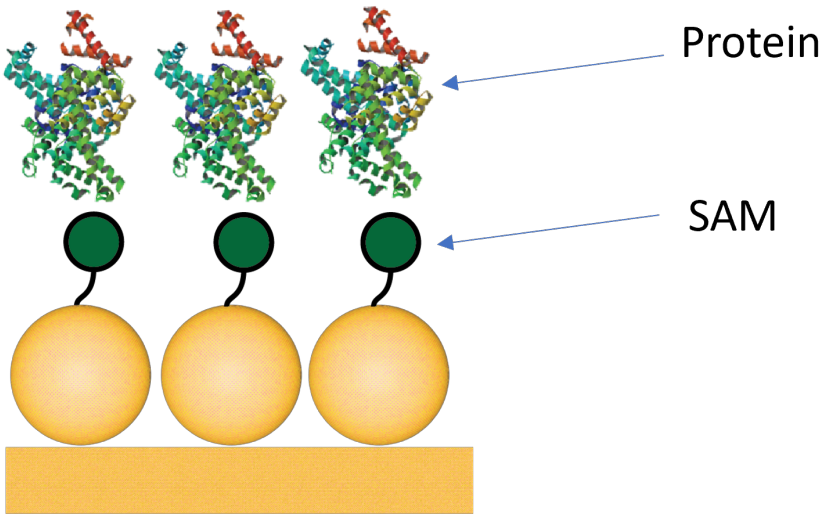


***Figure 8:*** *A schematic of a sample with a linking molecule between the nanoparticles and the protein.*

## 3.2 SERS Measurements

### 3.2.1 Solution measurements

During the project the choice was made to focus on measurements of proteins in solution, as this would be more comparable to real life applications. To measure a protein in solution a small layer of solution must be applied to the surface of the gold. However, just putting a small droplet on the surface has major drawbacks. First, the droplet evaporates quite quickly, especially if the chemical which is to be measured is dissolved in ethanol. Secondly, the droplet is not uniform in thickness across the surface of the gold film. To decrease evaporation and increase the uniformity of the solution layer a 3d-printed well was designed as can be seen in Figure 9. The procedure of preparing a sample for measuring is as follows. First, the gold film is attached to the bottom of the well with carbon-tape. Second, the well is filled with the protein solution and covered with a glass cover slip. Finally, the cover slip is pressed down, pushing out the excess solution. This process creates a thin, uniform layer of solution that does not evaporate quickly. The addition of a cover slip and a layer of solution unfortunately does add a lot of reflection and scattering. Due to the glass cover slip the laser light that gets to the sample is reflected by the air-glass and glass-solution interfaces. The addition of a solution means that the light that gets through the cover slip is scattered throughout the solution both ways. This means that the light that

reaches the gold film has greatly reduced in intensity, meaning that the signal is really weak. To combat the scattering the depth of the well was reduced to 0.3 $mm$, which was found to be the optimal height for a layer of carbon-tape, a layer of gold film and a thin layer of solution. Additionally, a different laser was used in the experiment, which increased the laser power that reaches the sample from about 90 µ$W$ to around 8 $mW$.

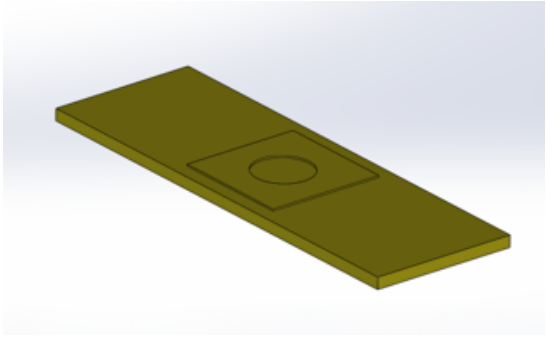

***Figure 9:*** *The well-design used for solution measurements.*

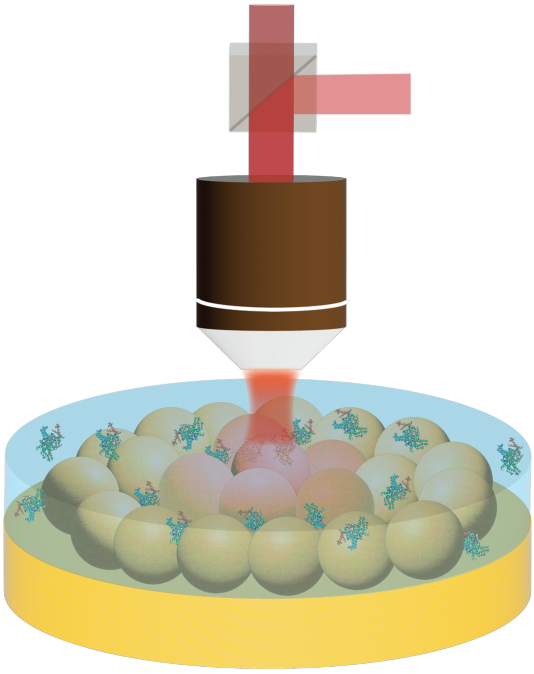

***Figure 10:*** *A schematic representation of measurements being done on the gold film with gold nanoparticles covered with a protein solution.*

### 3.2.2 Setup

The optical setup consists of an excitation source, a spectrometer and an optical microscope. The light starts its path at laser, the excitation source. The laser is a 500 $mW$ 640 $nm$ continuous-wave laser, of which the laser power is reduced to 420 $mW$ to increase stability. Due to the beam splitters and cleanup filter on the path the light takes the initial 420 $mW$ laser power is reduced to the around 8 $mW$ at the sample, as mentioned earlier. At the sample the beam is focused by a 100x magnifying 0.8 NA objective, focusing the light on a spot with a diamter of 700 $nm$. Next to the laser light a white light source can be used to perform darkfield imaging. The darkfield image shows the scattered light coming from the surface of the sample. This can be used to find aggregations of nanoparticles to perform measurements on. When the laser light reaches the sample it is reflected through the objective and passes through a beamsplitter in the direction of the spectrometer. Just before the spectrometer a notch filter is placed to remove the light with the same wavelength as the laser. The spectrometer has a range of 80 $nm$ in the positive and negative direction from the central wavelength. This wavelength was chosen to be 760 $nm$. This ensures that the fingerprint region of the proteins is contained within the measurements.

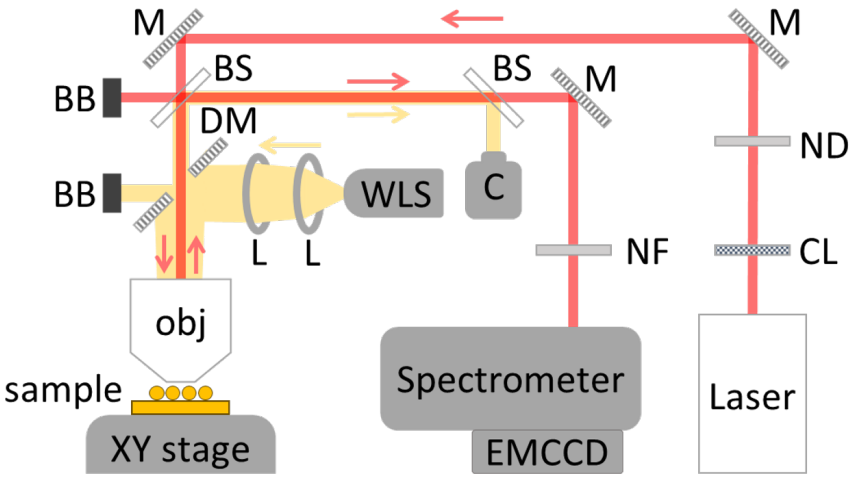


***Figure 11:*** *A visual representation of the optical setup used for the experiments.*

## 3.3 Data Analysis

### Extracting Spectra

One of the main drawbacks of measuring in solution is the fact that a lot of measurements won't show any protein signal. Thus the first part of analysis is extracting the individual measurements that contain useful signal. One of the ways an entire temporal scan can be visualized in one image is shown in the image below. In this image every individual scan is represented as a row in the y-axis, with the intensity represented by the color of the pixel. In these images the appearing and disappearing peaks from the proteins coming close to the gold nanoparticles can quickly be identified. That in turn makes it possible to quickly extract the spectra with signal, greatly streamlining the analysis process.

### Filtering and Peak Selection

When setting up the measurements both the background signal and the laser power at the sample are measured. The background signal is a measurement of the light surrounding the setup while the laseris off. This signal is subtracted from the raw measurements, leaving only the signal coming from the laser and its interactions with the sample. The laser power in $mW$ and the exposure time in $s$ are used for the normalization of the data. This analyzed data has the normalized unit of $Counts/mW/s$ and this data is used in the actual analysis. The analyzed spectra from the spectrometer contain noise which is characterized by a high frequency. A low-pass fourier filter is used to remove the high frequency noise and let the low frequency Raman signal pass. This Raman signal includes a broad background from the gold nanoparticles that have aggregated on the gold film. To remove this background a rolling average of the signal is taken and subtracted from the original signal. The signal strength that's left now hovers around zero with only the individual raman peaks reaching a substantial signal intensity. The individual peaks can now be extracted. Due to the high amount of peaks across the entire spectrum, a small range of wavenumbers is chosen to analyze. This range corresponds with the most dominant peak of the given protein. In this range the *findpeaks* function in Matlab is used to extract the wavenumbers and relative intensity of the first 5 peaks of any given spectrum, decreasing in intensity. For every combination of sample and protein solution the locations of these peaks are displayed in histograms to show the characteristics of these peaks across all measurements.

# 4 Results

In the following section the results of the experiments performed are presented. In the first three sections the 2 sample fabrication protocols are evaluated. In the final fourth section histograms are presented which visualize the measurements of protein solutions on bare gold and and MPA self-assembled monolayer. The final section presents 2 measurements performed on a sample funcionalized with cysteamine hydrochloride.

## 4.1 Measuring ultra low protein concentrations

Figure 12 shows three measurements of different, low concentration, BSA solutions. All measurements were done on a sample which was functionalized with an MPA SAM-layer with an exposure time of 100 $ms$ and 200 spectra per measurement.

In these images 3 important things stand out. The first thing is the bright broad band that is visible across all measurements from about 1400 to 1550 $cm^{-1}$. This broad band is really pronounced and does not align with the expectations of SERS background signal coming from the chemicals used to fabricate the sample. Secondly the intensity of the signal is similar for all 3 measurements even though the first measurement has a protein concentration more than 33 million times higher. The final important thing to note is the absence of the narrow raman peaks we expect for BSA, especially around the 1650 $cm^{-1}$ range where its most prominent peak should appear.

Due to the broad nature of the peak visible in these results the choice was made to increase the concentration drastically to try and overpower this broad signal. This broad peak had not appeared on any samples made with sample fabrication protocol 2, which does not use any acetone. Most likely there was a large layer of acetone on top of the gold nanoparticles that overpowered the protein signal. This is compounded by the fact that acetone has a broad raman peak around 1440 $cm^{-1}$. The choice was also made to reduce the amount of acetone used in the sample fabrication process to minimize the chance and magnitude of acetone signal appearing on other samples.

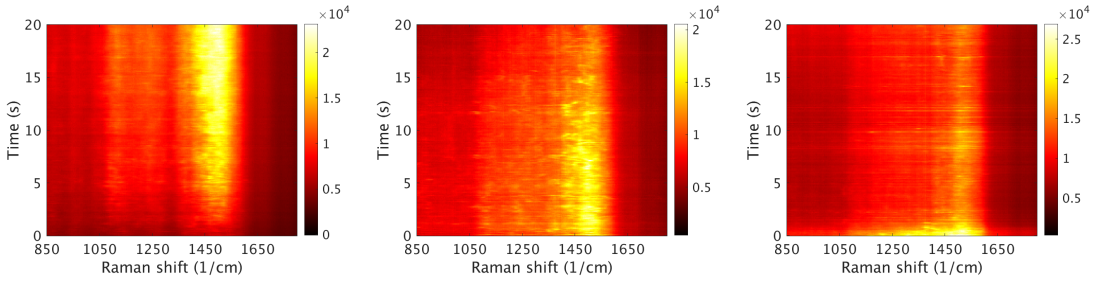


***Figure 12:*** *The 2D-images show the changing intensities of a full measurement of BSA solutions on gold nanoparticles with an MPA SAM-layer.* ***(a)****: 33nM BSA solution;* ***(b)****: 1 pM BSA solution;* ***(c)****: 1 fM BSA solution*

## 4.2 Concentration series of BSA

The histograms in Figure 13 show the frequency of peaks occuring in the signal in the range of 1600 through 1750 $cm^{-1}$. All histograms depict measurements done on a sample with a sam-layer of MPA. For all histograms the first 5 peaks were selected above a minimum peak height of 750 counts. Each of the histograms represent the combined spectra of all measurements done with a specific concentration of BSA.

When comparing the results from the dry sample, before the application of any protein solution, and the sample that had only been applied with water it becomes very clear that they are incredibly similar, both in their peak locations as the frequency with which the three peaks appear. The peak between 1675 and 1680 $cm^{-1}$ still appears at the 1 and 5 $mM$ concentrations, even though it has become less frequent. The same can be said about the peak around 1700 $cm^{-1}$, although this might not be significant. At the 1 $nM$ concentration the peak has shifted slightly to the range between 1665 and 1670 $cm^{-1}$.

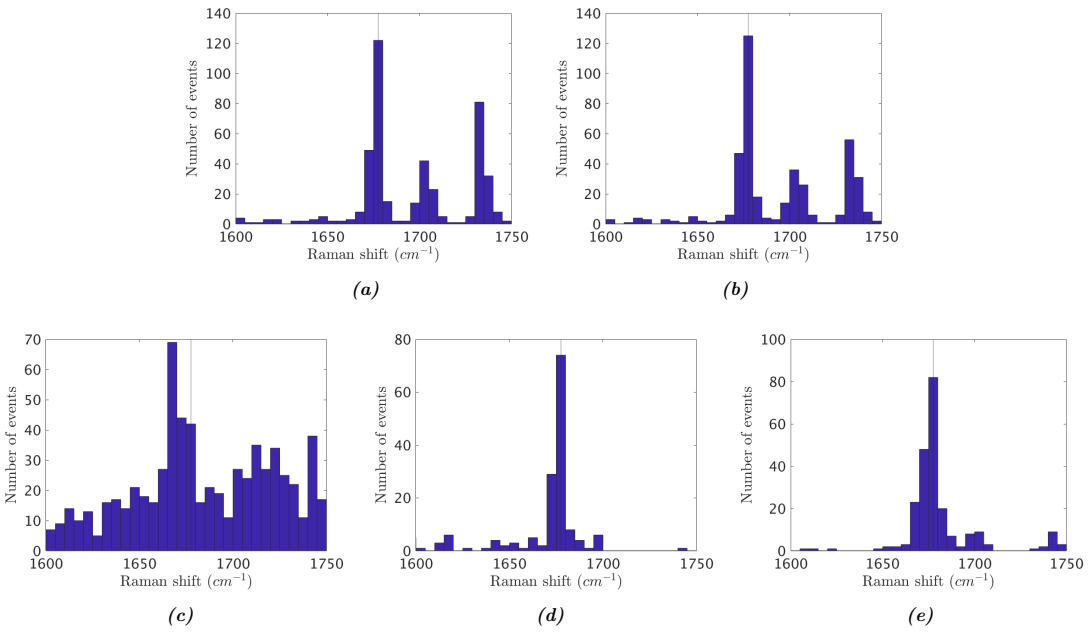


***Figure 13:*** *The histograms show the number of events of certain Raman shifts on gold aggregation with an MPA SAM-layer.* ***(a)****: Dry sample (200 spectra);* ***(b)****: Water (200 spectra);* ***(c)****: 1nM BSA solution (6500 spectra);* ***(d)****: 1 mM BSA solution (600 spectra);* ***(e)****: 5 mM BSA solution (800 spectra)*

## 4.3 Comparing fabrication protocols

The images in Figure 14 compare the results of a low acetone variation of fabrication protocol 1 to the results of a sample which used fabrication protocol 2. The lower acetone content was achieved by repeating four steps. First, the gold nanoparticle acetone solution was centrifuged as usual. Second, 1.5 $mL$ of the supernatant is removed. Thirdly, the safe-lock tube is refilled with 1.5 $mL$ of Milli-Q water. Finally, the solution is mixed thoroughly again. This process is repeated 3 times, thereby reducing the acetone concentration inside of the safe-lock tube to $\frac{1}{64}^{th}$ of the original solution. On top of that the 1.0 $mL$ of acetone used to start the aggregation of gold nanoparticles was replaced by the same volume of ethanol. The older fabrication was less efficient in creating larger aggregates as it did not use acetone to remove the citrate from the outside of the nanoparticles. The images show an individual analyzed spectrum from a longer measurement. All spectra were chosen to be comparable to the other spectra for those specific conditions. All measurements were done on bare gold aggregates without any linking molecule present with an exposure time of 100 $ms$.

With the dry spectra, before any protein solution application, it is immediately obvious that the signal strength of the protocol 1 sample is about 10 times higher than the signal strength of the sample made using fabrication protocol 2. This can be attributed to protocol 1 removing the citrates from the gold nanoparticles more completely and thus having better aggregates with a better enhancement factor. The measurement for protocol 1 still has two distinct broad peaks, one around 1300 and one around 1500 $cm^{-1}$. The one at 1500 $cm^{-1}$ is presumed to be the same as were present in the earlier measurements with the new fabrication process. On the protocol 2 sample two peaks are visible as well and are located at the same wavenumber as on protocol 1 sample. In both cases these peaks disappear when the protein solution is added and the expected broad background of gold nanoparticles appear. Even though this background disappeared and no protein solution was present 10 peaks were detected on the sample using protocol 1 at around 1680 $cm^{-1}$.

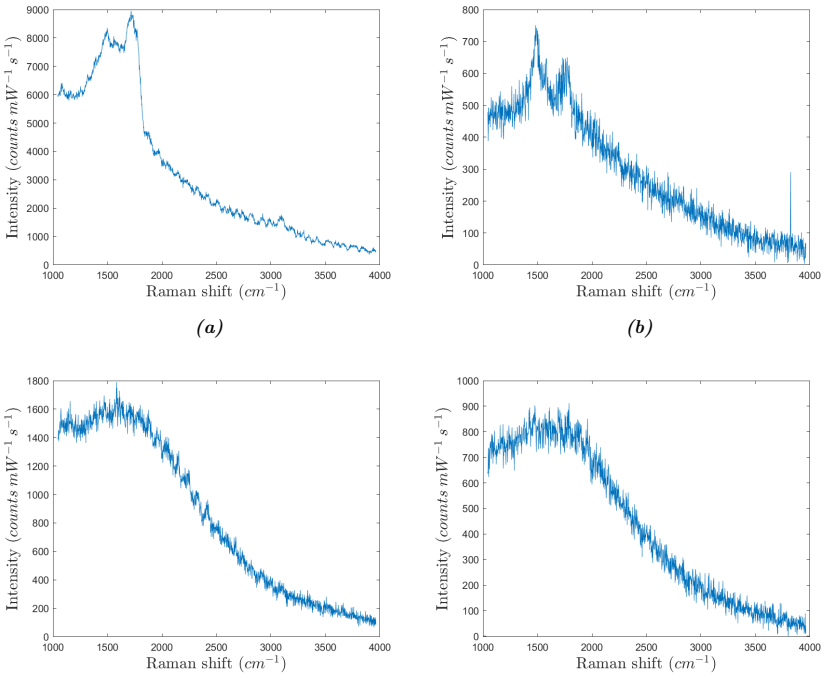


***Figure 14:*** *Four individual single raman spectra of two different fabrication protocols for a dry sample and a 1mM BSA solution.* ***(a)****: Low acetone fabrication protocol, dry;* ***(b)****: Old fabrication protocol, dry;* ***(c)****: Low acetone fabrication protocol, 1mM BSA solution;* ***(d)****: Old fabrication protocol, 1mM BSA solution*

## 4.4 Raman shifts of different proteins on different sample configurations

In Figure 15 the histograms show the frequency of peaks occurring in the signal from 1200 to 1750 $cm^{-1}$. For all the histograms the first 5 peaks were selected with a peak height higher than 20 percent of the peak of the broad background signal.

For the BSA solution on bare gold nanoparticles a really prominent peak can be seen between 1560 and 1590 $cm^{-1}$. A small peak can be distinguished between 1370 and 1380 $cm^{-1}$. Within the amide III band a peak can be seen between 1270 and 1280 $cm^{-1}$. For the Lysozyme solution on bare gold nanoparticles one primary peak is visible between 1550 and 1570 $cm^{-1}$. A small peak can be seen between 1370 and 1380 $cm^{-1}$. The spectrum also shows a broader peak between 1250 and 1280 $cm^{-1}$. When adding an MPA SAM-layer in between the gold nanoparticles and the BSA protein solution the highest peak becomes narrower and is located between 1580 and 1590 $cm^{-1}$. The small peak between 1370 and 1380 $cm^{-1}$ is still visible. In addition to these peaks a second prominent peak appears between 1340 and 1350 $cm^{-1}$. A small peak in signal can be seen between 1270 and 1280 $cm^{-1}$. For the Lysozyme solution on MPA the histogram is less clear and the peaks are less pronounced. Two broad peaks are visible, one between 1480 and 1500 $cm^{-1}$ and one between 1540 and 1560 $cm^{-1}$. The most prominent peak is the one between 1260 and 1280 $cm^{-1}$. Apart from a very small peak between 1360 and 1380 $cm^{-1}$ no other peaks can be distinguished.

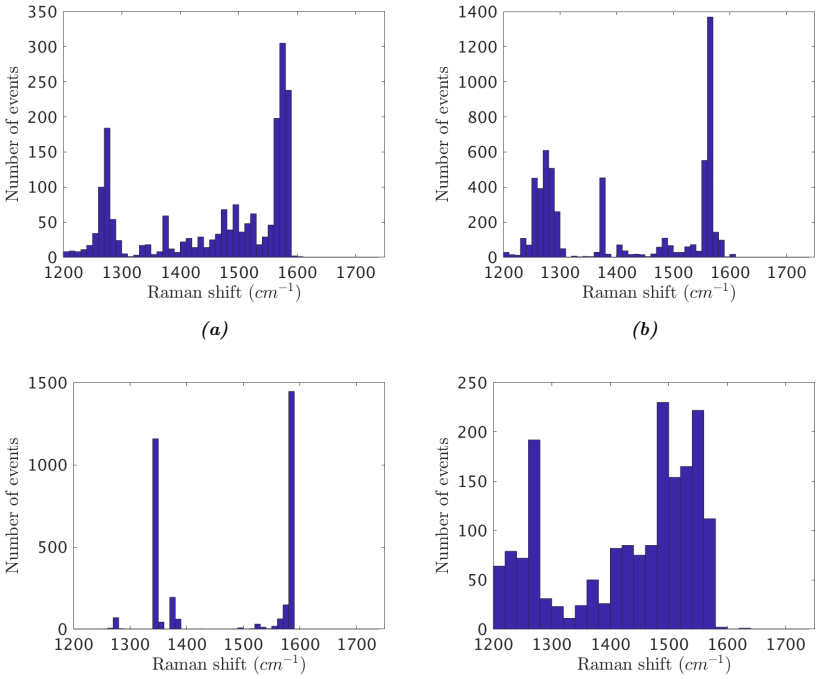


***Figure 15:*** *The histograms show the number of events of certain Raman shifts of two proteins on two different substrates.* ***(a)****: 1mM BSA solution on bare gold nanoparticles;* ***(b)****: 1mM Lysozyme solution on bare gold nanoparticles;* ***(c)****: 1mM BSA solution on MPA;* ***(d)****: 1mM Lysozyme solution on MPA*

Figure 16 shows three full measurements performed on different substrates with different protein solutions with an exposure time of 100 $ms$ and 200 spectra per measurement. The images in 16a and 16b show the peaks appearing and disappearing throughout the measurement. In Figure 16a a peak appears around 1500 $cm^{-1}$ at around 13 seconds into the measurement and disappear again around 18 seconds. In Figure 16b less pronounced peaks appears and disappears throughout the measurement around 1450 and 1500 $cm^{-1}$. These images show the diffusion of the protein solution across the sample's surface. When protein is close to the surface of the gold aggregation a peak appears and disappears again when it moves away. In Figure 16c a clear, distinct peak is visible between 1550 and 1600 $cm^{-1}$. This peak appears at the beginning and slowly disappears around 17 seconds into the measurement. The consistency of the position and intensity of the peak show that a BSA molecule got stuck on the MPA surface and moved away from the surface again at 17 seconds.

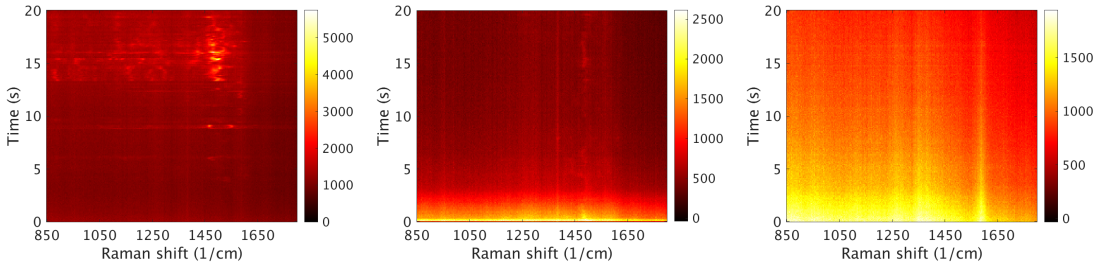


***Figure 16:*** *The 2D-images show the changing intensities of a full measurement of protein solution on different substrates. textbf(a): 1mM BSA solution on bare gold aggregates;* ***(b)****: 1mM Lysozyme solution on bare gold aggregates;* ***(c)****: 1mM BSA solution on MPA*

## 4.5 The use of Cysteamine hydrochloride as a linking molecule.

Experiments were also done using Cysteamine as a linking molecule. From these measurements two 2D-images are presented in Figure 17. These images show two measurements done on a dry sample before any measurements with a protein solution. In Figure 17a a broad background is visible throughout the measurement with a peak at around 1500 $cm^{-1}$. Figure 17b shows another measurement where narrow peaks appear and disappear across a broad range of raman shifts.

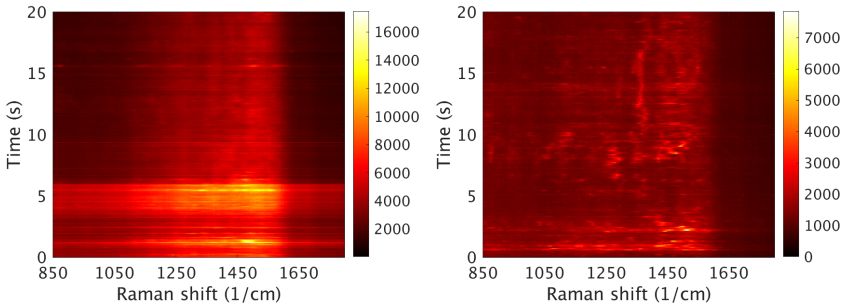


*(a)* *(b)*

***Figure 17:*** *The 2D-images show the changing intensities of a full measurement of a sample with no protein solution on gold nanoparticles with a Cysteamine SAM-layer.*

# 5 Discussion

## 5.1 Evaluating Sample Fabrication Protocol 1

The first three sections of the results presented the outcomes of the initial solution experiments performed on samples manufactured with sample fabrication protocol 1. In Section 4.1 a broad peak between 1400 and 1550 $cm^{-1}$ was presented across different measurements at extremely low protein concentrations. In Section 4.2 a single peak between 1675 and 1680 $cm^{-1}$ was found that is present across both dry samples and samples with a high protein solution on top of them. These two peaks, one broad peak between 1400 and 1550 $cm^{-1}$ and one narrow peak between 1675 and 1680 $cm^{-1}$, can both be attributed to acetone. Acetone namely has a broad raman peak around 1440 $cm^{-1}$ and a narrow raman peak around 1710 $cm^{-1}$.

In Section 4.3 a version of protocol 1 with a reduced aceton content is compared to protocol 2, which uses no aceton. The reduction of aceton reduces the effect of the prominent broad aceton peak that appears in earlier measurements using protocol 1 in solution measurements. With only a water solution on top of the gold aggregation the intensity of the broad background is similar in both Figure 14c and 14d. This can be attributed to the dilution of the gold nanoparticle solution. When removing the supernatant after centrifuging some of the gold nanoparticles are also removed. In the regular protocol, using 80 $nm$ nanoparticles, this is not the case, but for the modified low acetone sample smaller nanoparticles, namely 60 $nm$, were used which would need a longer centrifuging time. Repeating this process 3 times removed quite a large amount of nanoparticles. This was visible from the size of the gold layer that formed in the reaction chamber as well as under the darkfield microscope where the coverage of nanoparticles was similar to that of a sample made with protocol 2. On top of that there were still some peaks being detected with a wavenumber of around 1680 $cm^{-1}$, a peak which was earlier assigned to be coming from acetone. Because of the similar quality of aggregation and the small amount of aceton signal still being detected on samples fabricated using the modified version of protocol 1 the choice was made to use protocol 2 for all measurements of protein solutions. To fully utilize the high aggregation coverage and aggregation quality that protocol 1 can achieve a new protocol must be found to remove the aceton from the nanoparticle solution after the citrates have been removed.

## 5.2 Determination of vibrational bands

For the BSA solution on bare gold 2 peaks visible in the data can be assigned. The most prominent one of these was a relatively broad peak between 1560 and 1590 $cm^{-1}$. This broad peak can be assigned to both the Tryptophan and Phenylalanine peaks that appear around 1550 $cm^{-1}$ and 1586 $cm^{-1}$ respectively. The peak visible in the amide III band between 1270 and 1280 $cm^{-1}$ can be attributed to an $\alpha$-helix structure.

When the negative linking molecule MPA is used we see that the most prominent broad peak of the BSA becomes narrower and shifts slightly to 1580-1590 $cm^{-1}$. The contribution of Tryptophan to the broad peak visible on the bare gold disappears and only the Phenylalanine peak remains. When compared to the BSA on the bare gold the $\alpha$-helix peak between 1270 and 1280 $cm^{-1}$ almost disappears. The most pronounced change in the histogram is the appearance of a prominent peak between 1340 and 1350, which can be asssigned to Tryptophan.

A lysozyme solution on bare gold nanoparticles shows 2 peaks connected to protein structure. The most prominent peak, between 1550 and 1570 $cm^{-1}$ can be assigned to Tryptophan. The second one is a broad peak between 1250 and 1280 $cm^{-1}$. This peak can mainly be attributed to an $\alpha$-helix structure, with the shoulder around 1250 possibly coming from random structures within the protein. A second possibility for this shoulder is the polyproline II structure, a short helical structure too short to form a full $\alpha$-helix [26]. A peak from this structure would appear at 1252 $cm^{-1}$ [13].

When a negatively charged SAM-layer is added the most prominent narrow peak of the Lysozyme on bare gold disappears and a broad signal appears in the range from 1480 to 1560 $cm^{1}$. Within this range two peaks can be distinguished. The first one between 1460 and 1500 $cm^{-1}$ and the second one between 1540 and 1560 $cm^{1}$. The second one can be assigned to both Tryptophan and the amide II band, which both appear around 1550 $cm^{-1}$. There is no clear structural marker for protein structure between 1460 and 1500 $cm^{-1}$. It is possible that this peak is coming from the substrate itself and not the protein solution. The most likely candidate would be butylamine, which has a raman peak around 1460 $cm^{-1}$.

In all histograms a peak is visible around 1370 $cm^{-1}$. This peak is not a known marker for any part of protein structure, therefore it could not be assigned to the protein. Two raman-active molecules are

used in the protocol for aggregating the gold nanoparticles, ethanol and butylamine. Around 1370 $cm^{-1}$ butylamine is known to have 2 peaks around 1460 and 1300 $cm^{-1}$ [27]. In the same range ethanol has a slight peak around 1450 $cm^{-1}$ [28]. All three of these peaks are unable to cause the peak visible at 1370 $cm^{-1}$, the assignment of this peak therefore remains unknown. Another unknown peak appears in the histogram of MPA and lysozyme between 1480 and 1500 $cm^{-1}$ this could possibly be a peak coming from either ethanol or butylamine but this cannot be conclusively determined.

| **Protein + SAM** | **Raman Shift ($cm^{-1}$)** | **Assignments** |
|---|---|---|
| Bare Gold + BSA | 1270-1280 | $\alpha$-helix [10] |
| | 1370-1380 | Unknown |
| | 1560-1590 | Trp, Phe [19], [20] |
| Bare Gold + Lysozyme | 1250-1280 | $\alpha$-helix, random structure/polyproline II [10], [13] |
| | 1370-1380 | Unknown |
| | 1550-1570 | Trp [20] |
| MPA + BSA | 1270-1280 | $\alpha$-helix [10] |
| | 1340-1350 | Trp [20] |
| | 1370-1380 | Unknown |
| | 1580-1590 | Phe [19] |
| MPA + Lysozyme | 1260-1280 | $\alpha$-helix [10] |
| | 1360-1380 | Unknown |
| | 1480-1500 | Unknown |
| | 1540-1560 | Trp, Amide II [10], [20] |

***Table 2:*** *A list of Raman bands and their structures.*

When comparing the histogram of BSA to Lysozyme on bare gold, three things stand out. The first one is that the lysozyme histogram appears to have a peak possibly indicating random structure. Secondly, the prominence of the $\alpha$-helix peak is slightly higher for BSA than Lysozyme. Finally, the Lysozyme signal does not contain any Phenylalanine peaks and has a much more prominent peak for Tryptophan. All three of these phenomena are consistent with the fact that BSA has a higher $\alpha$-helix content than Lysozyme, Lysozyme contains more random structures and Lysozyme has many more Tryptophan residue groups than BSA.

An MPA SAM-layer greatly decreases the $\alpha$-helix peak visible in the BSA histogram. Additionally a peak appears around 1350 $cm^1$ assigned to Tryptophan, and the intensity of the Phenylalanine peak increases. The combination of these three changes can be explained by a change in secondary structure of the protein from a mostly $\alpha$-helix structure to a more $\beta$-sheet containing structure. This is because the $\beta$-sheet structure allows maximum space for large sidegroups like Tryptophan and Phenylalanine, making them more prominent in the raman signal [29]. This suggests the possibility of BSA aggregating when interacting with MPA.

Lysozyme does not show any conformational change from $\alpha$-helix to $\beta$-sheet when on an MPA SAM-layer. Its $\alpha$-helix peak does not reduce at all, nor does the peak of its most frequent side-group Tryptophan increase in prominence. One change that does happen is the disappearance of the distinguishable shoulder around 1250 $cm^{-1}$. It is most likely that the polyproline II helical structures disappear when on the negatively charged MPA because it was found that neutralization of Lysozyme's positively charged side-chains can induce $\alpha$-helix formation [30]. This would explain the diappearance of the shoulder and the increase of the $\alpha$-helix peak.

Section 4.5 shows the results from measurements performed on a dry sample functionalized with cysteamine hydrochloride. Both the broad background and the appearance of individual peaks could not be attributed to the cysteamine itself nor any raman-active molecules used in the sample fabrication process. The frequent appearance of both of these signals and the inconsistency of the peak location of the individual peaks would make it much more difficult to distinguish peaks coming from a protein in solution. Measurements done with a BSA solution also did not return any distinguishable peaks.

## 5.3 Recommendations

When it comes to sample fabrication protocol 1, two changes can be explored to decrease the amount of acetone present on the sample while keeping a high aggregation coverage. The first possibility is to improve the low acetone protocol used for the results in Section 4.3. The first improvement would be to try centrifuging the gold nanoparticle aceton mixture for longer with a higher centrifugal force. This would reduce the amount nanoparticles lost while removing the supernatant. The second improvement would be to dillute the solution even more often, to reduce the amount of aceton left in the final gold nanoparticle solution. A second change to the protocol that could be explored would be to expose the acetone solution to the air and let the acetone evaporate. Acetone evaporates much quicker at room temperature than the water in which the gold nanoparticles are dissolved. In a relatively short amount of time most of the acetone in the solution could have evaporated leaving only the gold nanoparticles, dissolved in water.

Due to the inconsistent nature of the gold nanoparticle aggregations of fabrication protocol 2 the absolute intensity of the different sample fabrications are unable to be compared properly. If fabrication protocol 2 is improved, a greater uniformity of aggregations across samples can be guaranteed. This would give rise to the possibility to compare the intensity of the signal and the frequency of events of protein coming close to the surface. Especially the interactions between charged proteins and charged SAM-layers would be able to be explored more thoroughly.

In this report only 2 proteins and 2 linking molecules were used to perform experiments on. In future research it would be interesting to look at other proteins and linking molecules to give a more complete picture of the different secondary structures and charges that proteins and linking molecules could have. It would be interesting to try to use a positively charged linking molecule other than Cysteamine. Cytochrome-C would be an interesting protein to study as it is a protein which has a distinct change in secondary conformation if structural changes occur. If the heme of the protein is exposed its $\alpha$-helix signature changes to a more $\beta$-sheet dominant signal. Proteins with more $\beta$-sheet dominated secondary structures or a protein dominated by random structures, like $\alpha$-synuclein, could be interesting to research.

# 6 Conclusion

In this research two different sample fabrication protocols were evaluated. Results show that the use of acetone in protocol 1 result in a broad peak between 1400 and 1500 $cm^{-1}$ and a narrow peak between 1675 and 1680 $cm^{-1}$. It was found that a reduction of acetone content in the fabrication protocol decreases the prominence of these peaks but also decreases the aggregation coverage of the gold nanoparticles. These factors makes protocol 1 currently unsuitable for SERS measurements of protein solutions, even though its aggregation coverage can be significantly better than protocol 2.

In the second part of this research the raman spectra of two proteins, BSA and Lysozyme, on top of bare gold and an MPA self-assembled monolayer were analyzed. It was found that the negatively charged MPA layer changed the structure of BSA from mostly $\alpha$-helix to a more $\beta$-sheet conformation. With lysozyme the negative charge of the MPA was found to interact with lysozyme's positively charged side-chains inducing $\alpha$-helix formation. It can be concluded that a negatively charged plasmonic surface can modify the vibrational modes of a protein in solution by changing its secondary structure. The influence of the net-charge of the protein and the charge of the plasmonic surface on the change in the protein's vibrational modes could not be fully studied.

Using cysteamine hydrochloride as a linking molecule showed both a broad peak and individual narrow peaks, even at dry conditions. These peaks were inconsistent and could not be assigned to the linking molecule itself or any other molecule used in sample fabrication. This inability to conclusively say what caused these peaks made cysteamine unsuitable for measurements with protein solutions.

# References


[1] K. A. Willets and R. P. Van Duyne, "Localized surface plasmon resonance spectroscopy and sensing," *Annu. Rev. Phys. Chem.*, vol. 58:267-97. No. ; Annu, 2007, ISSN: 0066-426X. DOI: 10.1146/annurev.physchem.58.032806.104607. eprint: 17067281.

[2] S. A. Maier, *Plasmonics: Fundamentals and Applications*. Springer US, 2007, ISBN: 978-0-387-37825-1. [Online]. Available: https://link.springer.com/book/10.1007/0-387-37825-1.

[3] P. L. Stiles, J. A. Dieringer, N. C. Shah, and R. P. Van Duyne, "Surface-enhanced Raman spectroscopy," *Annu. Rev. Anal. Chem. (Palo Alto Calif).*, vol. 1:601-26. No. ; Annu, 2008, ISSN: 1936-1335. DOI: 10.1146/annurev.anchem.1.031207.112814. eprint: 20636091.

[4] S. Schlücker, "Surface-enhanced Raman spectroscopy: concepts and chemical applications," *Angew. Chem. Int. Ed. Engl.*, vol. 53, no. 19, pp. 4756–4795, May 2014, ISSN: 1521-3773. DOI: 10.1002/anie.201205748. eprint: 24711218.

[5] F. Benz, R. Chikkaraddy, A. Salmon, *et al.*, "SERS of Individual Nanoparticles on a Mirror: Size Does Matter, but so Does Shape," *J. Phys. Chem. Lett.*, vol. 7, no. 12, pp. 2264–2269, Jun. 2016. DOI: 10.1021/acs.jpclett.6b00986.

[6] J. S. Rudra, S. H. Kelly, and J. H. Collier, "2.4 Self-Assembling Biomaterials73," in *Comprehensive Biomaterials II*, vol. 2, Walthm, MA, USA: Elsevier, Jan. 2017, pp. 67–89, ISBN: 978-0-08-100692-4. DOI: 10.1016/B978-0-12-803581-8.10210-3.

[7] Y. Kitagawa, D. Hobara, M. Yamamoto, and T. Kakiuchi, "Counterion binding induces attractive interactions between negatively-charged self-assembled monolayer of 3-mercaptopropionic acid on Au(111) in reductive desorption," *J. Solid State Electrochem.*, vol. 12, no. 4, pp. 461–469, Apr. 2008, ISSN: 1433-0768. DOI: 10.1007/s10008-007-0471-5.

[8] M. Oćwieja, J. Maciejewska-Prończuk, Z. Adamczyk, and M. Roman, "Formation of positively charged gold nanoparticle monolayers on silica sensors," *J. Colloid Interface Sci.*, vol. 501:192-201. Sep. 2017, ISSN: 1095-7103. DOI: 10.1016/j.jcis.2017.04.038. eprint: 28456103.

[9] C. Carnegie, J. Griffiths, B. de Nijs, *et al.*, "Room-Temperature Optical Picocavities below 1 nm3 Accessing Single-Atom Geometries," *J. Phys. Chem. Lett.*, vol. 9, no. 24, pp. 7146–7151, Dec. 2018. DOI: 10.1021/acs.jpclett.8b03466.

[10] N. Kuhar, S. Sil, and S. Umapathy, "Potential of Raman spectroscopic techniques to study proteins," *Spectrochim. Acta, Part A*, vol. 258:119712. Sep. 2021, ISSN: 1873-3557. DOI: 10.1016/j.saa.2021.119712. eprint: 33965670.

[11] S. Cai and B. R. Singh, "Identification of $\beta$-turn and random coil amide III infrared bands for secondary structure estimation of proteins," *Biophys. Chem.*, vol. 80, no. 1, pp. 7–20, Jul. 1999, ISSN: 0301-4622. DOI: 10.1016/S0301-4622(99)00060-5.

[12] N. Kuhar, S. Sil, T. Verma, and S. Umapathy, "Challenges in application of Raman spectroscopy to biology and materials," *RSC Adv.*, vol. 8, no. 46, pp. 25 888–25 908, Jul. 2018, ISSN: 2046-2069. DOI: 10.1039/C8RA04491K.

[13] S. Dolui, A. Mondal, A. Roy, *et al.*, "Order, Disorder, and Reorder State of Lysozyme: Aggregation Mechanism by Raman Spectroscopy," *J. Phys. Chem. B*, vol. 124, no. 1, pp. 50–60, Jan. 2020, ISSN: 1520-6106. DOI: 10.1021/acs.jpcb.9b09139.

[14] B. Jachimska and A. Pajor, "Physico-chemical characterization of bovine serum albumin in solution and as deposited on surfaces," *Bioelectrochemistry*, vol. 87, pp. 138–146, Oct. 2012, ISSN: 1567-5394. DOI: 10.1016/j.bioelechem.2011.09.004.

[15] K. Murayama and M. Tomida, "Heat-Induced Secondary Structure and Conformation Change of Bovine Serum Albumin Investigated by Fourier Transform Infrared Spectroscopy," *Biochemistry*, vol. 43, no. 36, pp. 11 526–11 532, Sep. 2004, ISSN: 0006-2960. DOI: 10.1021/bi0489154.

[16] J. J. Babcock and L. Brancaleon, "Bovine serum albumin oligomers in the E- and B-forms at low protein concentration and ionic strength," *Int. J. Biol. Macromol.*, vol. 53, pp. 42–53, Feb. 2013, ISSN: 0141-8130. DOI: 10.1016/j.ijbiomac.2012.10.030.

[17] V. Vetri, F. Librizzi, M. Leone, and V. Militello, "Thermal aggregation of bovine serum albumin at different pH: comparison with human serum albumin," *Eur. Biophys. J.*, vol. 36, no. 7, pp. 717–725, Sep. 2007, ISSN: 1432-1017. DOI: 10.1007/s00249-007-0196-5.

[18] T. Topală, A. Bodoki, L. Oprean, and R. Oprean, "Bovine Serum Albumin Interactions with Metal Complexes," *Clujul Medical*, vol. 87, no. 4, p. 215, 2014. DOI: 10.15386/cjmed-357.

[19] B. Hernández, F. Pflüger, S. G. Kruglik, and M. Ghomi, "Characteristic Raman lines of phenylalanine analyzed by a multiconformational approach," *J. Raman Spectrosc.*, vol. 44, no. 6, pp. 827–833, Jun. 2013, ISSN: 0377-0486. DOI: 10.1002/jrs.4290.

[20] H. Takeuchi, "Raman structural markers of tryptophan and histidine side chains in proteins," *Biopolymers*, vol. 72, no. 5, pp. 305–317, Jan. 2003, ISSN: 0006-3525. DOI: 10.1002/bip.10440.

[21] B. Sjöberg, S. Foley, B. Cardey, and M. Enescu, "An experimental and theoretical study of the amino acid side chain Raman bands in proteins," *Spectrochim. Acta, Part A*, vol. 128, pp. 300–311, Jul. 2014, ISSN: 1386-1425. DOI: 10.1016/j.saa.2014.02.080.

[22] P. He, Y. Zhang, L. Liu, W. Qiao, and S. Zhang, "Ultrasensitive SERS Detection of Lysozyme by a Target-Triggering Multiple Cycle Amplification Strategy Based on a Gold Substrate," *Chem. Eur. J.*, vol. 19, no. 23, pp. 7452–7460, Jun. 2013, ISSN: 0947-6539. DOI: 10.1002/chem.201203224.

[23] N. R. Agarwal, M. Tommasini, E. Ciusani, A. Lucotti, and P. M. Ossi, "Protein-Metal Interactions Probed by SERS: Lysozyme on Nanostructured Gold Surface," *Plasmonics*, vol. 13, no. 6, Dec. 2018, ISSN: 1557-1963. DOI: 10.1007/s11468-018-0728-0.

[24] S. Strazdaite, E. Navakauskas, J. Kirschner, T. Sneideris, and G. Niaura, "Structure Determination of Hen Egg-White Lysozyme Aggregates Adsorbed to Lipid/Water and Air/Water Interfaces," *Langmuir*, vol. 36, no. 17, pp. 4766–4775, May 2020, ISSN: 0743-7463. DOI: 10.1021/acs.langmuir.9b03826.

[25] A. Steudle and J. Pleiss, "Modelling of Lysozyme Binding to a Cation Exchange Surface at Atomic Detail: The Role of Flexibility," *Biophys. J.*, vol. 100, no. 12, p. 3016, Jun. 2011. DOI: 10.1016/j.bpj.2011.05.024.

[26] Z. Shi, C. A. Olson, G. D. Rose, R. L. Baldwin, and N. R. Kallenbach, "Polyproline II structure in a sequence of seven alanine residues," *Proc. Natl. Acad. Sci. U.S.A.*, vol. 99, no. 14, pp. 9190–9195, Jul. 2002. DOI: 10.1073/pnas.112193999.

[27] *Butylamine(109-73-9) Raman spectrum*, [Online; accessed 24. Jan. 2024], Jan. 2024. [Online]. Available: https://www.chemicalbook.com/SpectrumEN_109-73-9_Raman.htm.

[28] *Ethanol(64-17-5) Raman spectrum*, [Online; accessed 24. Jan. 2024], Jan. 2024. [Online]. Available: https://www.chemicalbook.com/SpectrumEN_64-17-5_Raman.htm.

[29] J. Dawson, *Protein Secondary Structure*, [Online; accessed 28. Jan. 2024], Jan. 2021. [Online]. Available: https://ecampusontario.pressbooks.pub/bioc2580/chapter/protein-secondary-structure.

[30] A. L. Rucker and T. P. Creamer, "Polyproline II helical structure in protein unfolded states: Lysine peptides revisited," *Protein Science : A Publication of the Protein Society*, vol. 11, no. 4, p. 980, Apr. 2002. DOI: 10.1110/ps.4550102.